Single Event Upsets for Space Shuttle Flights of New General Purpose Computer Memory Devices

P. M. O'Neill and G. D. Badhwar

Abstract—**The replacement of magnetic core with a well characterized semiconductor memory in the Space Shuttle orbiter general purpose computers (GPC's) has provided a wealth of on-orbit radiation effects data since 1991. The fault tolerant GPC's detect, correct, and downlink memory upset status and orbiter position information every few seconds, giving us the ability to correlate 1400 upsets to date with altitude, geomagnetic latitude, and solar conditions. The predicted upset rate was computed by a modified path-length distribution method. The modification accounts for the Weibull distribution cross-section (rather than a single upset threshold) and the device sensitive volume thickness. Device thickness was estimated by the method normally used to account for edge effects at the upset cross-section discontinuity that occurs at ion changes. A galactic cosmic ray environment model accurately models the average particle flux for each mission. The predicted and observed upset rates were found to be in good agreement for sensitive volume thicknesses consistent with the device's fabrication technology.**

Introduction

THE ability to accurately predict the rate of single event upsets (SEU) in space borne computer memories directly affects costs not only for new designs but also for enhancements to existing systems. Fortunately, the prediction methodology has continued to improve. Particle accelerator test data has become more readily available as more test facilities have become operational. Cosmic ray models are now more representative of actual environments. However, there are still computational limitations that render the methodology less than perfect. There are no operating particle facilities capable of penetrating components edge-on, so upset rate measurements greater than about sixty degrees cannot be made. This requires some flexibility in choosing a method for convoluting the SEU cross-section curve to the environment. Compared with the accelerator, the space environment consists of a much broader energy spectrum of many ion species. This can produce "surprises" on-orbit, such as multibit upsets, that may not be seen at an accelerator. Also, the environment at the component depends on accurate particle transport calculations which require an accurate spacecraft shielding distribution.

Manuscript received October, 1993; revised March, 1994.

The authors are with National Aeronautics and Space Administration, Johnson Space Center, Houston, TX 77058.

IEEE Log Number 9401247.

To further reduce these uncertainties, actual upset rate data from spacecraft is needed for comparison with analytical predictions. However, there are few opportunities where well known experimental conditions for a large enough set of data are available to allow accurate comparison. The Space Shuttle flights of new general purpose computer (GPC) memory devices provide an excellent "test fixture" for evaluating SEU prediction methodologies.

Space Shuttle General Purpose Computers

The five Space Shuttle general purpose computers (GPCs) which are the heart of each Space Shuttle orbiter's guidance, navigation, and flight control system were upgraded in 1991. The original magnetic core GPC memories were replaced by new microelectronic devices made by Inmos Corp.—the IMS1601EPI. The IMS1601EPI is a non-radiation hardened 64kx1 static random access memory (SRAM) built using a conventional four-transistor cell approach and 1.3 micron complementary metal oxide semiconductor (CMOS) technology. As part of the GPC design process, this technology was tested both in space and in the laboratory. These investigations determined that, like most nonradiation hardened SRAM's, it was susceptible to single event upsets (SEU's) in the natural space radiation environment the Shuttle operates in [1]. The GPC's were therefore designed with a modified Hamming Error Detection and Correction (EDAC) code [2] and periodic memory scrubbing which detects (up to two bitflips per word) and corrects (up to one bitflip per word) SEU's before they can contaminate the data processing system. The GPC's record the time of each soft error the EDAC finds and downlinks it along with the GPC affected. This information is retrieved after each mission and correlated with the actual ground track to determine the location of each upset. Each GPC has 200 pieces of the IMS1601EPI 64kx1 SRAM arranged to form a $2 \times (2 \times 128\text{ k} \times 25)$ mainstore memory array. The array's 25-bit output word format is composed of 16 data bits, 6 check bits, and 3 store-protect bits. The 16 data and 6 check bits (22 total) are routed to the SEC-DED circuitry and can therefore be monitored for single event upsets during each scrub cycle (1.6789 s intervals). This provides a total of $2 \times (2 \times 128\text{ k} \times 22) = 11{,}534{,}336$ memory bits

TABLE I
SUMMARY OF SHUTTLE GPC UPSETS

STS	Launch Date, Duration	Altitude (nmi)	Number* of SEU's	Comments	Deceleration** Parameter, ϕ
		28.5 degree inclination missions			
37	April 5, 1991, 6 days	243	55	Many SAA upsets	1300
43	August 2, 1991, 9 days	160	44	1 Pre-MECO upset	1443
44	November 24, 1991, 7 days	200	31		1116
49	May 7, 1992, 9 days	200	60	Many SAA upsets	1042
50	June 25, 1992, 14 days	160	61		942
46	July 31, 1992, 8 days	230, 160	77	Many SAA upsets	934
52	October 22, 1992, 10 days	165	50	1 Pre-MECO upset	787
54	January 13, 1993, 8 days	165	52		768
55	April 26, 1993, 10 days	165	45	1 Pre-MECO upset	729
57	June 21, 1993, 10 days	250	130	Many SAA upsets	798
51	Sept. 12, 1993, 10 days	160	65		701
		57.1 degree inclination missions			
39	April 29, 1991, 8 days	140	99	1 eleven-bit SEU	1277
48	September 12, 1991, 5 days	292	161	Many SAA upsets	1525
42	January 22, 1992, 5 days	163	75	1 Pre-MECO upset	1290
45	March 24, 1992, 8 days	165	81		1050
47	September 12, 1992, 8 days	165	111	1 fourteen-bit SEU	855
53	December 2, 1992, 7 days	180	141	Only 2 upsets within SAA	811
56	April 8, 1993, 9 days	165	115		729

*Actual number of upsets reported by GPC's includes multi-bit upsets.
**Deceleration parameter is discussed in Radiation Environment section.

(equivalent to 11 Mb or 1.375 MB) per GPC which can be monitored in real time during flight.

Fig. 1 shows the location of each SEU detected for each of the first eighteen flights following the maiden flight of the new GPC's in April 1991. The new GPC's have logged over 1400 SEU's without a single inflight anomaly due to radiation. About half of these upset's occurred for 28.5 degree inclination missions (Figure 1a) and the other half were for 57.1 degree flights (Fig. 1(b)) as summarized in Table I.

For both 28 and 57 degree missions, higher SEU concentrations are found in the South Atlantic Anomaly (SAA) and at the higher latitudes. Most SAA upsets are thought to be caused by protons trapped in the van Allen belts which happen to dip closer to the earth's surface in the region east of South America. SAA upsets are observed only for altitudes above about 200 nmi. Five of the 28.5 degree flights had altitudes of at least 200 nautical miles and only one of the 57.1 degree inclination flights was above 200 nautical miles (see Table I).

Outside the SAA, most upsets are thought to be caused by galactic cosmic rays (GCR's) that penetrate the geomagnetic field. GCR upsets are concentrated toward higher latitudes because lower rigidity (particle momentum/charge) particles can penetrate the field at higher latitudes. The geomagnetic cutoff effect is more pronounced for the 57 degree flights since the cutoff rigidity varies roughly as the cosine of the geomagnetic latitude raised to the fourth power.

The upset rate prediction method for heavy ions is different than for protons. Therefore, to allow finer discrimination of model features, upsets caused by GCR particles are separated from those caused by SAA protons. Observed upsets were separated by assuming that each upset that occurred within the SAA was due to trapped protons except the nominal GCR background found outside the SAA was allowed to overlay the SAA. These observed SEU rates, identified as either GCR or SAA upsets, are compared with model predictions later.

PRE-MAIN ENGINE CUTOFF (MECO) SEU'S

Four (4) SEU's have occurred prior to main engine cutoff (MECO is about 8.5 minutes after liftoff) as shown in Fig. 1. These Pre-MECO SEU's were at altitudes around 300,000 ft. Experiencing upset's this early after liftoff is not surprising since the heavy ion flux is essentially the same above 200,000 ft as it is at orbital altitudes, and the shuttle is above 200,000 ft within three minutes of liftoff. The high magnetic latitude of the launch site (Fig. 1), for both 28 or 57 degree flights, enhances the ascent upset rate probability.

Multibit Upsets

Multibit upsets—more than one bit affected by a cosmic ray ion—represent about 7% of the SEU's for 57 degree flights, and 3% of the SEU's for the 28.5 degree flights. Most of the multibit upsets involve a pair of bits. However, some involve triplets and quadruples. There was one case where over eleven (11) bits were upset and another where fourteen (14) were upset by a single cosmic ray. These rare cases happened at latitudes of 57 degrees and 52 degrees, respectively, and multibit upsets in general occur more frequently at high latitudes (see Fig. 1). In all cases, the EDAC successfully dealt with the multibit events. The EDAC is implemented so that each GPC word is composed of bits from different chips. Therefore if a highly ionizing cosmic ray encompasses several con-

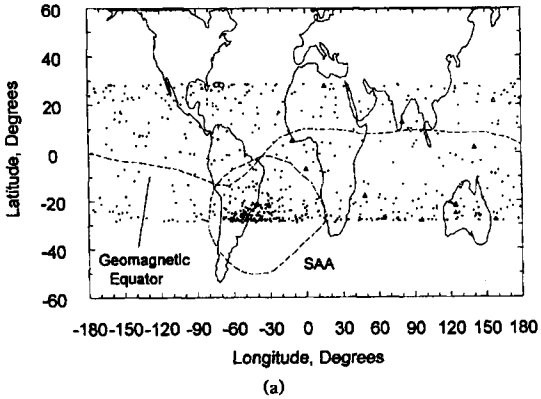

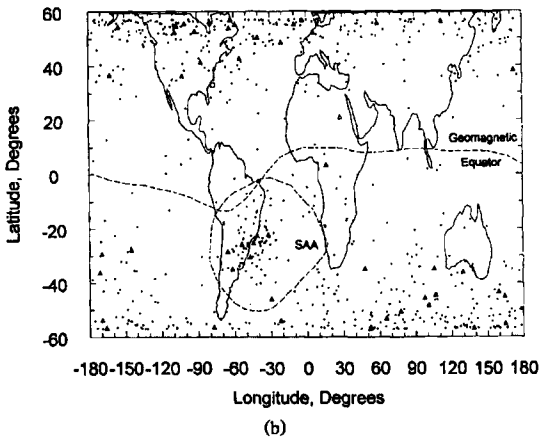

Fig. 1. Shuttle GPC single event upsets. Multibit SEU's are indicated by triangles and Pre-MECO upsets are indicated by squares. Note that a greater proportion of the multibit upsets are in the SAA and at higher geomagnetic latitude for the 57 degree as opposed to the 28.5 degree inclination missions. (a) Shuttle GPC single event upsets for 28.5 degree inclination orbits. (b) Shuttle GPC single event upsets for 57.1 degree inclination orbits.

tiguous bits in a chip, the EDAC can detect it since each affected bit occupies a different word. These findings are consistent with multibit hits being due to higher linear energy transfer (LET) particles such as those slower, more charged ions that can only penetrate the geomagnetic field at the higher magnetic latitudes.

Most of the multibit upsets affected only one memory area (low or high) and are assumed to be in one chip. However, there have been cases where apparently more than one chip was hit by a single particle. On STS-43 GPC #1 lo and hi memory were hit simultaneously and STS-48 had two cases where different chips were upset simultaneously: GPC #1 lo and #2 hi, and GPC #4 lo and #1 lo.

These results indicate the importance of accurately predicting inflight performance of a new chip prior to system design. The remainder of this paper describes the prediction methodology used for the IMS1601EPI and

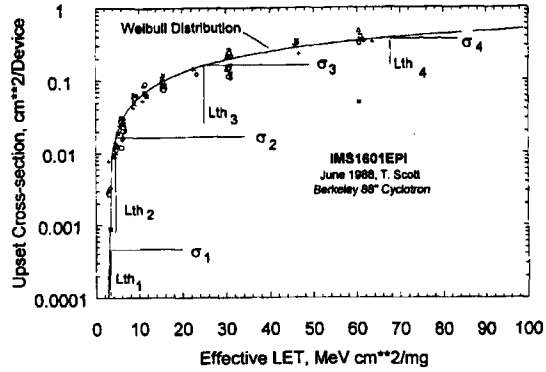

Fig. 2. Heavy ion single event upset integral cross-section versus effective linear energy transfer (LET) for seven IMS1601EPI devices tested at Berkeley 88" cyclotron [3]. The Weibull distribution $(\sigma(L) = 1 - \exp\{-[(L - L_{th})/W]^s\}$ for $L > L_{th}$ and 0 for $L < L_{th}$) is fit by the following parameters: $L_{th} = 2.75$, $W = 140.0$, and $s = 0.95$). The heavy ion single event upset cross-section curve is approximated by multiple thresholds and cross-section intervals.

compares predicted with actual flight results for the first eighteen shuttle flights of the new GPC's.

Single Event Upset Methodology

Before flight of the new GPC's, the memory device (IMS1601EPI) was tested for SEU and latchup susceptibility to heavy ions at the Berkeley 88" cyclotron [3] and to protons at the Harvard Cyclotron [4]. In this device, upsets may be caused by two distinct processes: 1) the original ion (usually a galactic cosmic ray) deposits energy by ionization directly in the sensitive volume (this process is henceforth referred to as direct ionization); and 2) energy is deposited by heavy ions that are produced in the device as fragments of proton–nuclei interactions (this process is henceforth referred to as proton secondary upsets and the trapped protons of the South Atlantic Anomaly are usually the source).

Direct Ionization Methodology

The upset rate is computed in principle using the well-known method of convoluting the radiation flux with the path-length distribution [5] and cross-section of a rectangular parallelepiped (RPP) sensitive volume. However, the original method allows only one RPP sensitive volume. Since the actual cross-section is not a step function but varies with effective LET, it has been suggested [6] that the cross-section be divided into several steps in order to more accurately represent it (see Fig. 2). This is like assuming that several sensitive volumes are present, each with different upset thresholds (Lth_i) and cross-sections (σ_i). Again, this method assumes the sensitive volume is thin (relative to its width). This solves the problem of integrating over all solid angles because the integration can be terminated at L_{max} if the cross-section is saturated at high effective LET (i.e., high angles of incidence). For the IMS1601EPI, the cross-section is essentially saturated for an L_{max} of about 50–100 MeV cm^2/mg (Fig. 2).

The direct deposition SEU rate per device (in SEU's/second) is the sum of the SEU rate of each step and is given by

SEU Rate (direct deposition)

$$= \pi \sum_{i=1}^{n} \left\{ A_i Lth_i t_i \int_{L_{\min_i}}^{L_{\max}} D[s_i(L)] I(L) L^{-2}\, dL \right\}, \quad (2)$$

where,

i is the step index ranging from 1 to the number of steps (n),

Lth_i is the effective LET threshold for the ith step in MeV cm^2/mg,

A_i is the surface area of the ith sensitive volume in m^2 ($A_i = 10^{-4}\,\Delta\sigma_i$)

$\Delta\sigma_i = \sigma_i - \sigma_{i-1}$ is the upset cross-section step size ($\sigma_0 = 0$) in cm^2/device, the cross-section for the IMS1601EPI is in Fig. 2

t_i is the thickness of the ith sensitive volume in g/cm^2, t_i is assumed to be a fixed fraction of the ith sensitive volume width where the width is the square root of the cross-section step ($\sqrt{\Delta\sigma_i}$). t_i is converted from cm to g/cm^2 by multiplying the density of silicon (2.33 g/cm^3),

$L_{\min_i} = Lth_i t_i / \text{smax}_i$ is the minimum LET (MeV cm^2/mg) required to upset the part by passing across it diagonally,

smax_i is the largest path-length (the diagonal) found in the ith sensitive volume (in g/cm^2),

$L_{\max}$ is the effective LET (MeV cm^2/mg) where the cross-section becomes saturated,

$D(s_i(L))$ = differential path-length distribution [5] in the ith sensitive volume in $(\text{g/cm}^2)^{-1}$, $s_i(L)$ is the path-length within which an ion of LET, L, will deposit enough energy within the sensitive volume to upset it ($s_i(L) = Lth_i t_i / L$), and

$I(L)$ is the radiation environment LET spectrum (the integral LET flux of ionizing particles) at the device and is determined in the next section in number of ions/(meter^2 steradian second).

Upset Cross-Section

The IMS1601EPI device used in the GPC's is the epitaxial substrate version, since the commercial version is susceptible to latchup and therefore is not acceptable for GPC application. Heavy ion testing confirmed that the epitaxial version did not latchup for linear energy transfer (LET) values up to 100 MeV cm^2/mg [1]. The measured SEU cross-section versus effective LET is shown in Fig. 2. The cross-section represents an upset susceptibility for particles of a given effective LET. The effective LET is by definition the true LET divided by the cosine of the angle of beam incidence. Hence, the assumption that the sensitive volume is a thin slab is inherent in Fig. 2. The IMS1601EPI upset cross-section is accurately represented by the integral Weibull distribution [8]:

$$\sigma(L) = 1 - \exp\left\{-[(L - L_{th})/W]^s\right\} \cdot \text{for } L > L_{th} \text{ and 0 for } L < L_{th}, \quad (1)$$

with the following parameters: $L_{th} = 2.75$, $W = 140.0$, and $s = 0.95$ as shown in Fig. 2. Weibull parameters were found by simply plotting the function and the data and varying the parameters until the function fits the data.

Device Sensitive Volume Thickness to Width Ratio

To select the thickness (t_i) for each step, one ratio of sensitive volume thickness to width (P_k) is used. The sensitive volume is assumed to be square and very thin. This allows t_i to be found from $t_i = P_k \sqrt{\Delta\sigma_i}$, where P_k is always chosen to be small. Provided $P_k \ll 1$ the upset rate is not very sensitive to P_k, and a value of 1/1000 (or smaller) leads to an upper bound on the upset rate [7]. Selecting the correct ratio P_k is similar to having to pick a single part thickness using the original, single rectangular parallelepiped upset rate formulation since part thickness is not measured in radiation part testing. The value of P_k can be estimated based on the device technology. However, we present here a novel approach based on the edge effect that distorts the cross-section curve at high incidence angles. Since P_k is small this is a small effect and the measurements are somewhat subjective we cannot rely on it entirely and it may not apply to all devices. However, in this case, the edge effect determination of P_k is consistent with other methods as will be seen below.

Edge Effect Determination of P_k

The value of P_k was estimated from a careful examination of the upset cross-section curve versus effective LET. Typically a part is exposed to higher angles of incidence (θ) to increase the effective LET. Then, a higher LET particle is chosen at normal incidence ($\theta = 0$) to further increase the LET and so on. If the sensitive volume is not too thin, the effective area of the chip will be reduced by more than the cos θ factor since ions passing through the edges will not have sufficient LET to upset the part. This effect can be accounted for using the following equation [8]:

$$\sigma(\theta = 0) = \sigma(\theta) \cos\theta / (\cos\theta - P_k \sin\theta). \quad (3)$$

This equation can easily be solved for the desired ratio (P_k):

$$P_k = [1 - \sigma(\theta)/\sigma(0)]/\tan\theta \quad (4)$$

Fig. 3 shows the actual data points for a typical IMS1601EPI chip of the seven samples tested [3]. In this case, four different ions were used at incidence angles from zero to about 60 degrees to span the effective LET range shown (a laser beam was used to insure there was no shadowing of the beam at 60 degrees incidence [3]). Note that the cross-section discontinuity at each change of ions can be measured. We computed P_k for thirteen ion transition, cross-section discontinuity points for the seven IMS1601EPI test samples. The value of P_k ranged from 0.1–0.2 with a mean of 0.16 ± 0.04. Just as important as the value of P_k is that P_k was found to be

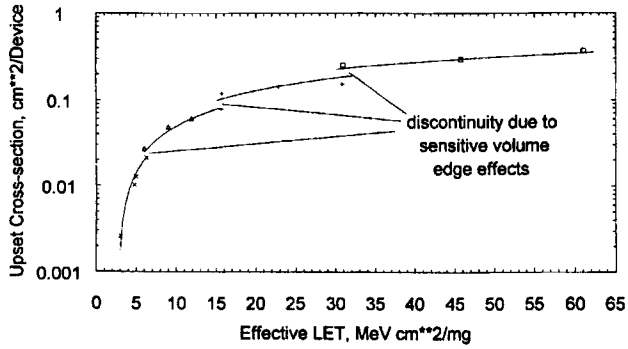

Fig. 3. Upset cross-section measurements for a typical one of the seven IMS1601EPI chips tested clearly showing the cross-section discontinuity at high incidence angles due to the finite thickness of the sensitive volume. The cross-section values and the incidence angle at the discontinuity determines the sensitive volume thickness to width ratio (P_k).

independent of LET because this is an important assumption of the model.

This value is consistent with the physical characteristics of the device. Dividing the measured limiting cross-section (about 0.5 cm^2) shown in Fig. 2 by the number of transistors in the device (65,536 bits, 4 transistors per bit) yields a transistor area of 190 μm^2. If this sensitive area is 1.3 μm thick (the IMS1601EPI is a 1.3 μm technology device) the P_k is 0.09, reasonably consistent with the edge effect estimate.

Proton Secondaries

The measured SEU cross-section for protons is shown in Fig. 4. The cross-section represents an upset susceptibility for protons of a given energy. The SEU rate is computed for the expected Shuttle trapped proton environment (J) which is described in the next section. The upset rate (due to proton secondaries) is computed in principle by folding the radiation flux with the measured upset cross-section.

SEU Rate (proton secondaries)

$$= 4\pi \int_0^{E_{max}} \sigma_p(E) J(E)\, dE \quad (5)$$

where,

$J(E)$ is the differential proton flux at the sensitive volume defined in the next section in number of protons/(cm^2 steradian second MeV/n),

$\sigma_p(E)$ is the proton cross-section (see Fig. 4) in cm^2/device as a function of energy (not LET as for heavy ions), and

E_{max} is the highest energy of the proton spectrum (about 500–1000 MeV/n).

Radiation Environment

The heavy ion radiation environment for shuttle flights consists of high energy galactic cosmic rays (GCR's) that penetrate the earth's magnetosphere and lower energy protons that are trapped by the magnetosphere.

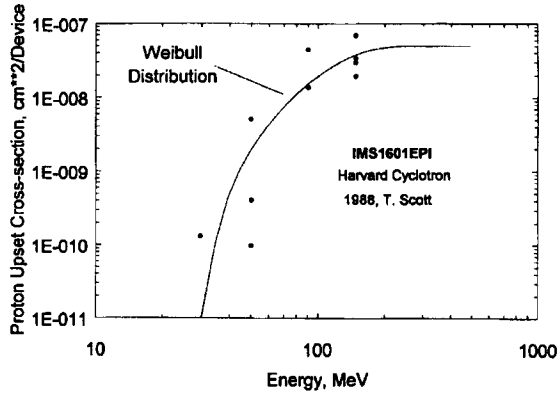

Fig. 4. Differential single event upset cross-section versus energy for proton beam based on Harvard cyclotron testing [4]. The Weibull distribution ($\sigma_p(L) = 1 - \exp\{-[(L - L_{th})/W]^s\}$ for $L > L_{th}$ and 0 for $L < L_{th}$) is fit by the following parameters: $L_{th} = 30.0$, $W = 100.0$, and $s = 2.00$).

Galactic Cosmic Ray

The standard GCR model often used to predict upset rates is the Cosmic Ray Effects on Microelectronics (CREME) code [9]. However, the CREME code accounts for solar cycle modulation using an 11 year cyclic function of time and does not distinguish between odd-even cycles which have a 22 year period. The model presented below depends on the actual Climax neutron monitor count for a given time (rather than time alone) and agrees more accurately with actual GCR flux measurements from 1954 to present. The new model agrees with the actual GCR flux measured over the past 4 solar cycles within 9.2% [10]. The CREME code differs most at odd solar minima and achieves an overall accuracy of 30.6% for the same forty year period [10].

The free-space GCR component at earth is the result of a solar wind modulated local interstellar spectrum (LIS), i.e., the GCR spectrum at the outer boundary of the heliosphere (roughly 100 AU). The GCR component in the vicinity of earth is described by the time stationary

diffusion-convection model of solar modulation [11]. This model has been successful [12], [13] in describing the variation in galactic cosmic rays with time, given the deceleration parameters (solar wind velocity, diffusion coefficient, and size of modulation cavity). This precisely determines the modulated GCR component at earth given the value of the deceleration parameter (ϕ) which varies over the 22-year solar cycle [14].

Since ϕ is a direct measure of the magnitude of solar modulation, it is correlated with the ground-level (mountain) measurement of neutron flux which also responds to solar modulation. Since the Climax neutron monitor responds to higher energy cosmic rays (proton energy greater than 2.2 GeV) than those that are responsible for upsets in spacecraft avionics (energy below 1 GeV/nucleon), the Climax neutron count can be used to predict the lower energy cosmic ray modulation.

The following model [14] provides accurate ($\pm 10\%$) GCR flux based on the Climax neutron monitor count. The deceleration parameter (ϕ) is determined 95 days later than the Climax neutron count by the following correlation equations:

$$\phi(T) = -0.8124\,\text{Climax}(\text{T} - 95\text{ d}) + 3957.89 \quad (6a)$$

$$\phi(T) = -0.8563\,\text{Climax}(\text{T} - 95\text{ d}) + 4202.76 \quad (6b)$$

$$\phi(T) = -0.9528\,\text{Climax}(\text{T} - 95\text{ d}) + 4772.86, \quad (6c)$$

where Climax(T − 95 d) is the Climax neutron monitor count (averaged over ± 14 d) at a time 95 d earlier than current time (T). This time delay is consistent with the results of the time-dependent diffusion-convection model which suggests that propagation times are on the order of 100 d for reasonable values for the solar wind velocity, the diffusion coefficient, and the radius of the modulating boundary [15]. The value of ϕ is then used in the diffusion-convection model (the Fokker–Planck equation) to propagate the LIS through the heliosphere to the vicinity of the earth.

These model equations for ϕ were found [14] by determining the value of ϕ that produced the best fit to the quiet time cosmic ray energy spectra (see Fig. 5) for many balloon and satellite measurements gathered over three solar cycles. The resulting correlation in Fig. 6 shows the model predictions consistently lie close to the actual measurements over a forty year period.

The value of solar modulation associated with each shuttle mission was found using this model. Table I shows the resulting value of ϕ for each shuttle mission since the new GPC's were introduced in 1991. These values are used in the Fokker–Planck equation to determine the GCR differential energy flux for each mission. The differential energy flux is converted to integral LET flux [9] based on the known stopping power versus energy for each element.

Magnetospheric Attenuation

Free-space GCR's are attenuated by the earth's magnetosphere. The cosmic ray's cutoff rigidity (particle momentum/charge) determines its ability to penetrate the magnetic field and reach a given position. Shea and Smart [16] have modeled the earth's magnetic field and tabulated the cutoff rigidity for each magnetic latitude and longitude. Adams [17] has combined this table with an orbit trajectory code to determine the cutoff for each point of the orbit. Averaging over the orbit results in an effective cutoff rigidity transmittance function which is used to attenuate the free space cosmic ray flux.

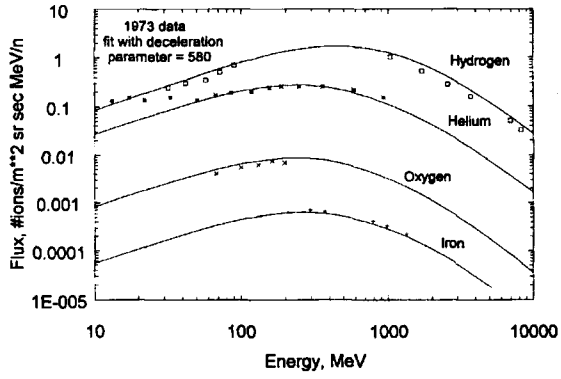

Fig. 5. Differential energy spectra for hydrogen, helium, oxygen, and iron for 1973. Data points are actual particle measurements taken by high altitude balloons and satellites such as IMP-8 [23]–[25]. Smooth curves are the best fit by the GCR model equations described in the text for $\phi = 580$ (near solar minimum).

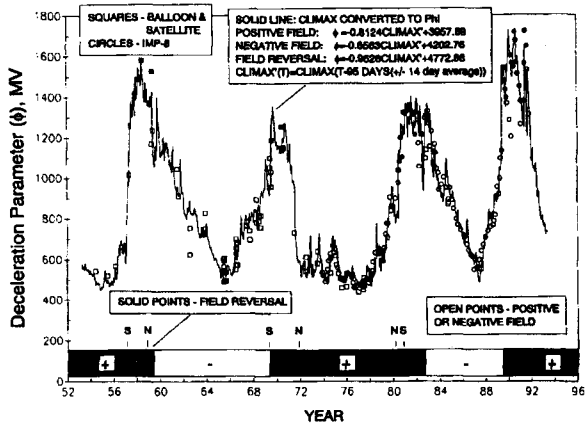

Fig. 6. Deceleration parameter (ϕ) versus time for past forty years based on the actual Climax neutron count [26] using (6) which converts the Climax neutron count to ϕ. Data points were determined by fitting actual balloon and/or satellite quiet-time cosmic ray flux with the GCR model equations described in the text.

Trapped Proton Radiation Environment

The trapped radiation spectrum during solar maximum is determined by the AP-8 model with the 1970 epoch and the 1970 USC & GS magnetic field [18]. Only trapped protons are considered since orbiter shielding is sufficient at the GPC's to eliminate trapped electrons. The orbit

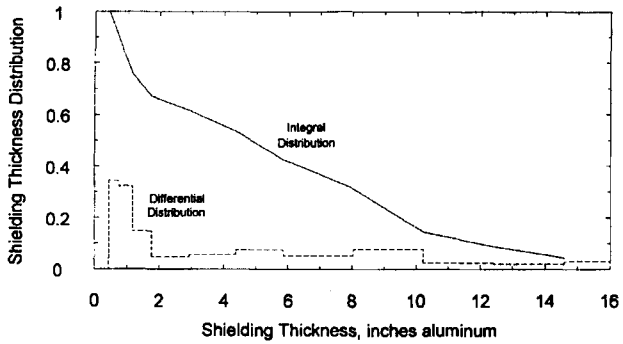

Fig. 7. Orbiter shielding distribution at the GPC location in aluminum equivalent mass thickness based on the elemental volume dose program [21].

averaged proton energy spectrum propagated through the orbiter walls increases dramatically with altitude. Missions with altitudes above about 200 nautical miles have significant trapped proton contributions. Even for these flights, the only trapped proton contribution occurs over the South Atlantic Anomaly—consistent with actual SEU's logged on high altitude missions (Fig. 1). The orbit averaged proton flux within the orbiter for 28.5 and 57.1 degree inclinations is similar.

Particle Transport Through Shuttle Orbiter Walls

The GCR and trapped proton energy spectra outside the spacecraft are propagated through the spacecraft walls by assuming energy loss due to ionization and nuclear collisions [19] for a given wall thickness. The propagated energy spectrum at the device is then converted to an LET spectrum [9] since direct ionization calculations (2) require an integrated LET spectrum $I(L)$. Orbiter shielding is accounted for by generating an LET spectrum for ten (10) different thicknesses that cover the range of thicknesses for the GPC location in the orbiter. The orbiter shielding distribution in the forward avionics bay where the GPC's are located was calculated using the elemental volume dose program [20]. The aluminum equivalent thickness of the orbiter body was determined for 968 rays uniformly distributed in all directions emanating from the location of the GPC's [21]. The distribution is approximated by ten (10) thicknesses as shown in Fig. 7. The LET flux for each of the ten thicknesses is a linear combination of the flux for each thickness weighted in proportion to the shielding distribution in Fig. 7.

This approach yields satisfactory results for thicknesses of 10 g/cm^2 (1.5 in). However, nuclear fragments are not accounted for, so the model underestimates the flux for large thicknesses. Adams [19] has shown that the errors become significant for shielding of 50 g/cm^2 (7.3 inches aluminum) and more. About 70% of the orbiter shielding is above 10 g/cm^2 and 35% is above 50 g/cm^2.

Predicted Versus Actual Upset Rate

The frequency of SEU's varies considerably as a function of position within the orbit. Fig. 8 shows the time between actual GPC upsets for a typical high altitude, high inclination orbit (STS-48). For this orbit, about half of the upsets are located over the South Atlantic Anomaly. The time between upsets decreases by 2–3 orders of magnitude, as the shuttle traverses the SAA. Thus, upsets caused by the GCR particles are easily separated from those caused by trapped protons by assuming each SAA upset was due to trapped protons, allowing for the normal GCR background to overlay the SAA.

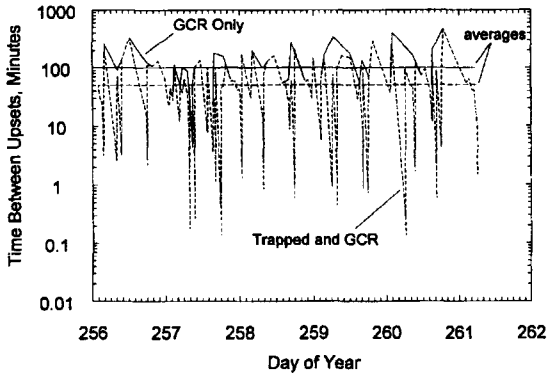

Fig. 8. Time between upsets for a typical high altitude (292 nmi), high inclination (57.1 degrees) mission (STS-48) showing that the upset rate can increase several orders of magnitude during SAA passage.

Predicted Versus Actual Upset Rates—GCR

The actual SEU rate due to GCR's was calculated by dividing the total number of GCR upsets by the flight time for each of the eighteen STS missions. This data appears in Fig. 9(a). The points around 1–3 upsets/GPC day are the 28.5 degree missions and the higher upset rates (4–7 upsets/GPC day) are the 57.1 degree inclination missions.

The predicted SEU rate due to GCR's was determined using the integrated pathlength distribution method (2). The average free-space GCR flux was determined for each shuttle mission based on the deceleration parameter

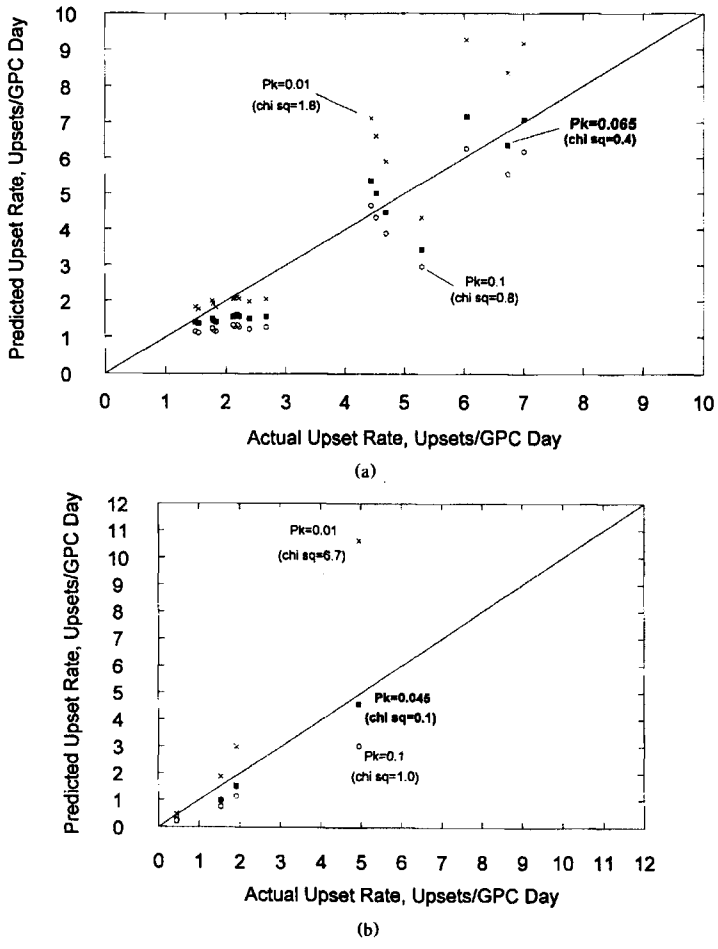

Fig. 9. Predicted versus actual upset rates for shuttle missions showing that best correlation is found for sensitive volume thickness to width ratio (P_k) of about 0.05 ± 0.01. For GCR upsets the best correlation is found for sensitive volume thickness to width ratio (P_k) of about 0.065, and for SAA upsets it is found to be about 0.045. (a) Predicted versus actual upset rate for GCRs. (b) Predicted versus Actual Upset Rate for Trapped Protons.

(see ϕ in Table I) derived from the average Climax neutron count during the mission. The average GCR flux at the device (I(L)) was found by propagating the free-space flux through the earth's magnetosphere and the spacecraft shielding as described in the radiation environment section above.

Fig. 9(a) shows the predicted upset rates for several values of the device geometry parameter which describes the sensitive volume thickness to width ratio (P_k). Note that the larger value ($P_k = 0.1$) produces the lower predicted upset rates and the smaller value ($P_k = 0.01$) produces the higher predicted upset rates. This is because the minimum LET that can produce an upset is proportional to P_k. A value of about 0.065 for P_k was found to give the best correlation between predicted and actual GCR upset rates. The smallest correlation coefficient (chi sq = 0.4) was found for $P_k = 0.065$ but this seems to be dominated by the higher inclination flights since the 0.01 value produces better agreement for the lower inclination flights.

The fact that one value of P_k cannot be found to satisfy both the 28.5 and 57.1 degree flights may be due to the inaccuracies of the transport code discussed earlier. Since the code underestimates target fragmentation effects, the computed LET flux for 28.5 degree orbits may have more error than the 57 degree orbits. This is believed to be because the lower inclination heavy ion spectra consist of more energetic particles which produce more fragmentation than the 57 degree orbits. We observed this effect [22] in the LET distribution measured by the Tissue Equivalent Proportional Counter (TEPC) flown on STS-51 (28.5 degree) and STS-56 (57.1 degree). The model underestimated the LET distribution for both missions, but, for LET's above minimum ionizing iron nuclei the model grossly underestimates the flux for the STS-51 (28.5 de-

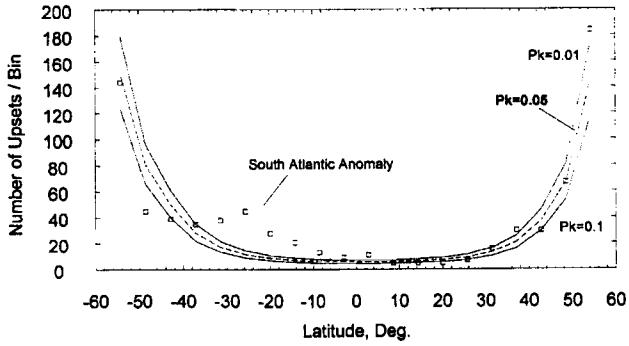

Fig. 10. Distribution of upsets with geodetic latitude. Actual distribution (squares) obtained from the 629 upsets observed for the seven 57 degree STS missions. The predicted distribution (lines) is based on averaging the predicted upset rate over geodetic longitude for each latitude bin (5.7 degrees of latitude) then multiplying by the actual total number of GPC-Days of the flights. The average predicted Deceleration Parameter (980) for the time period of the flights was assumed. The sensitive volume ratio (P_k) ranging from 0.01 to 0.1 fits the actual data.

gree) mission. This suggests that the true value of P_k is larger than 0.065, more consistent with the 0.16 ± 0.04 value determined from the edge effect measurement.

Predicted Versus Actual Upset Rates—Trapped Protons

The actual SEU rate due to trapped proton's was calculated by dividing the total number of trapped proton upsets by the flight time for each of the four STS missions with altitudes above 200 nmi. This data appears in Fig. 9(b). The points below 2 upsets/GPC day are the 28.5 degree missions (STS-37, 49, and 57) and the higher upset rates (around 5 upsets/GPC day) is the 57.1 degree inclination mission (STS-48). The upset rates are higher for the 57.1 degree inclination mission (STS-48) mainly because its altitude is higher than the 28.5 degree missions (STS-37, 49, and 57), but also the 57.1 degree orbit samples the heart of the SAA where the proton flux is greater.

The method used to predict SEU rate due to trapped protons differs from that described above for GCR upsets. Trapped protons cause upsets by both direct ionization and secondary particles created by the trapped protons interacting with chip material. In this case the proton flux $J(E)$ determines the environment. The upset rate due to direct ionization of these particles is found by (2) just as was done for GCR's. However, the upset rate due to secondaries is found by (5). Fig. 9(b) shows the predicted upset rate for several values of P_k from 0.01 to 0.1 to show the sensitivity to P_k. The contribution of secondaries does not depend on the P_k ratio; however, the direct ionization contribution does. The correlation is practically ideal (chi sq = 0.1) for a sensitive volume thickness to width ratio of 0.045.

Latitude Dependence

Fig. 10 shows the actual distribution of upsets with geodetic latitude obtained from all of the upsets observed for the 57 degree STS missions. For comparison with the model, the predicted distribution is also shown. The predicted distribution is based on averaging the predicted number of upsets over geodetic longitude for each latitude bin. The average predicted Deceleration Parameter ($\phi = 980$) for the time period of the flights was assumed. The sensitive volume ratio (P_k) ranging from 0.01 to 0.1 fits the actual data very well.

Conclusions

An integration method has been presented for processing particle accelerator upset cross-section data to predict in-flight SEU rates. The method was applied to a well defined set of actual upset rate data—the new memory device used by the STS orbiter. A special effort was made to ensure accurate knowledge of environmental conditions. A galactic cosmic ray model, accurate to $\pm 10\%$, was used to define the actual radiation environment during each of the eighteen STS flights analyzed.

The method has proven to be capable of accurately predicting upset rate provided the geometric parameter that describes the ratio of sensitive volume thickness to width (P_k) for the device is known. It was demonstrated that P_k determined by observing the edge effect discontinuity (that occurs in measured cross-section versus effective LET at the transition from high angle of incidence to zero when a new, usually heavier ion is selected) is consistent with device technology. The value of P_k for the IMS1601EPI was determined to be about 0.1 based on edge effect measurements (0.16) and comparison of predicted and actual upset rates (0.05), and is consistent with the dimension derived from device technology (0.09). An exact shielding calculation would increase the predicted upset rate and make the value of P_k determined from comparison of predicted and actual upset rates (0.05) more consistent with edge effect measurements and device technology. In any case, the results of this study strongly suggest that P_k is not close to the limiting value of 0.001 or 0.0001.

Acknowledgments

We thank Dr. Roger Pyle of the Enrico Fermi Institute, University of Chicago, for providing the Climax neutron

monitor data which is necessary to determine the galactic cosmic ray spectrum. We also wish to extend our appreciation to Tom Scott of the International Business Machines company for providing results of his heavy ion and proton single event upset testing.

REFERENCES

[1] A. H. Taber, A. V. Gillow, and R. E. Dickinson, "Space Shuttle general purpose computer radiation effects study—1991 Update," IBM Report 91-L75-001, February 26, 1991.

[2] M. Y. Hsiao, "A class of optimal minimum odd-weight-column SEC-DED codes," *IBM J. Res. Develop.*, 14, 395–401, July 1970.

[3] T. Scott, Private communication, 1989.

[4] ——, "Cosmic ray upset experiment results," IBM Report 89-PN6-023, November 8, 1989.

[5] J. C. Pickel, and J. T. Blandford Jr., "Cosmic-ray-induced errors in MOS devices," *IEEE Trans. Nucl. Sci.*, vol. NS-27, pp. 1006–1015, 1980.

[6] E. L. Petersen, J. B. Langworthy, and S. E. Diehl, "Suggested single event upset figure of merit," *IEEE Trans. Nucl. Sci.*, vol. NS-30, 1983.

[7] D. Chlouber, P. O'Neill, and J. Pollock, "General upper bound on single event upset rate," *IEEE Trans. Nucl. Sci.*, vol. NS-37, p. 1065, 1990.

[8] E. L. Petersen, J. C. Pickel, J. H. Adams, Jr., and E. C. Smith, "Rate predictions for single event effects—a Critique," *IEEE Trans. Nucl. Sci.*, vol. NS-39, pp. 1577–1599, 1992.

[9] J. H. Adams Jr., "Cosmic Ray Effects on Microelectronics, Part IV," Naval Research Laboratory Memorandum Report 5901, December 31, 1986.

[10] G. D. Badhwar and P. M. O'Neill, "An improved model of galactic cosmic rays for space exploration missions," *Nuclear Tracks and Radiation Measurements*, vol. 20, pp. 403–410, 1992.

[11] E. N. Parker, *Interplanetary Dynamical Processes*, New York; Wiley, 1963.

[12] L. A. Fisk, "Solar modulation of Galactic Cosmic rays, 2," *Journal of Geophysical Research*, vol. 76, p. 221, 1971.

[13] M. Garcia-Munoz, J. A. Simpson, T. G. Guzik, J. P. Wefel, and S. H. Margolis, "Cosmic ray propagation in the galaxy and in the heliosphere: The path-length distribution of low energies," *Astrophys. J. Suppl. Series*, vol. 64, pp. 269–304, May 1987.

[14] Badhwar, G. D. and P. M. O'Neill, "Time Lag of Twenty Two Year Solar Modulation," Proceedings of the International Cosmic Ray Conference, SH 6.21, Calgary, July 19–30, 1993.

[15] O'Gallagher, "A time-dependent diffusion-convection model for the long-term modulation of cosmic rays," *Astrophys. J.*, vol. 197, pp. 495–507, April 15, 1975.

[16] M. A. Shea and D. F. Smart, Report No. AFCRL-TR-75-0185, Hanscom, AFB, MA, 1975.

[17] J. H. Adams Jr., J. R. Letaw, and D. F. Smart, "Cosmic ray effects on microelectronics, Part II: The geomagnetic cutoff effects," Naval Research Laboratory Memorandum Report 5099, May 26, 1983.

[18] D. M. Sawyer and J. I. Vette, "AP8 Trapped proton Environment for Solar Minimum and Solar Maximum," National Space Science Data Center Report NSSDC/WDC-A-R & S 76-06, NASA-GSFC TMS-72605, December 1976.

[19] J. H. Adams Jr., "The variability of single event upset rates in the natural environment," *IEEE Trans. Nucl. Sci.*, vol. NS-30, pp. 4475–4480, 1983.

[20] S. C. Hamilton and B. Liley, Rockwell International Document No. SD 76-SA-0184-1, 1976.

[21] W. Atwell, E. R. Beever, and A. Hardy, "Radiation shielding analysis for the Space Shuttle Program: An Overview," Presented at the Nuclear Society Topical Conference on Theory and Practices in Radiation Protection and Shielding, Knoxville, TN, April 22–24, 1987.

[22] G. D. Badhwar, F. A. Cucinotta, L. A. Braby, and A. Konradi, "Shuttle measurements of LET spectra and comparison with radiation transport models," Submitted to Radiation Research, vol. 139, pp. 344–350, 1944.

[23] M. Garcia-Munoz, G. M. Mason, and J. A. Simpson, "The anomalous ^{4}He component in the cosmic-ray spectrum < 50 MeV per nucleon during 1972–1974," *Astrophys. J.*, vol. 202, pp. 265–275, 1975.

[24] W. R. Webber, "The Energy Spectra of the Cosmic Ray Nucleonic and Electronic Components," *Proc. of the 13th Int. Cosmic Ray Conf.*, vol. 5, pp. 3568–3614, University of Colorado, Denver, 1973.

[25] M. Garcia-Munoz, M. E. Juliusson, G. M. Mason, P. Meyer, and J. A. Simpson, "Energy dependence of the Si/Fe ratio in the galactic cosmic rays," *Astrophys. J.* vol. 197, pp. 489–493, 1975.

[26] R. Pyle, Private communication, 1993.